Journal of Thermal Stresses
Publication details, including instructions for authors and subscription information:
http://www.informaworld.com/smpp/title~content=t713723680

BUCKLING OF AUTOMATIC TRANSMISSION CLUTCH PLATES DUE TO THERMOELASTIC/PLASTIC RESIDUAL STRESSES

Nadine Audebert [a]; J. R. Barber [a]; P. Zagrodzki [a]
[a] Department of Mechanical Engineering and Applied Mechanics, University of Michigan, Ann Arbor, Michigan, USA

Online Publication Date: 01 April 1998

To cite this Article Audebert, Nadine, Barber, J. R. and Zagrodzki, P.(1998)'BUCKLING OF AUTOMATIC TRANSMISSION CLUTCH PLATES DUE TO THERMOELASTIC/PLASTIC RESIDUAL STRESSES',Journal of Thermal Stresses,21:3,309 — 326
To link to this Article: DOI: 10.1080/01495739808956149
URL: http://dx.doi.org/10.1080/01495739808956149

BUCKLING OF AUTOMATIC TRANSMISSION CLUTCH PLATES DUE TO THERMOELASTIC/PLASTIC RESIDUAL STRESSES

Nadine Audebert
J. R. Barber
P. Zagrodzki
Department of Mechanical Engineering and Applied Mechanics
University of Michigan
Ann Arbor, Michigan, USA

THIS ARTICLE IS DEDICATED TO RICHARD B. HETNARSKI ON THE OCCASION OF HIS SEVENTIETH BIRTHDAY.

The plates of multidisk automatic transmission are known to buckle under extreme operating conditions. Axisymmetric (coning) and nonaxisymmetric (potato chip) modes can be obtained. It is shown that these modes result from in-plane axisymmetric residual bending moments in the disk and the critical value for each mode is found. A numerical algorithm is then developed to determine the residual moment due to a prescribed axisymmetric thermal history. Allowance is made for the temperature dependence of yield stress, elastic modulus, and coefficient of thermal expansion. The results show that susceptibility to buckling depends on a dimensionless geometric shape factor, the material properties, and the magnitude of the largest thermal excursion. With steel disks and typical design values for the shape parameter, buckling is predicted for temperature differences of about 600°C between inner and outer radii.

The plates of multidisk automatic transmissions often exhibit signs of thermal damage upon disassembly. Typical indications include "leopard spotting," in which spots on the disk surface are discolored and may show signs of surface melting or dragging of softened material, and "thermal banding," in which the discolored regions consist of axisymmetric bands around the surfaces. In addition, the disassembled disks are often found to be permanently deformed out of plane [1, 2]. This deformation commonly occurs in one of two modes. One is a "coning" mode (Figure 1), in which the out-of-plane deformation is axisymmetric and the initially plane annular disk is deformed into a section of a truncated conical surface [2, 3]. The other is the "potato chip" or "pringling" mode (Figure 2), in which the deformed disk has a saddle shape corresponding to sinusoidal deformations around the circumference with wavenumber $N = 2$. If a coned disk is cut radially from

Received 10 November 1997; accepted 10 November 1997.
The authors are pleased to acknowledge support from the Raybestos Products Company and from the National Science Foundation under contract number CMS-9619527.
Address correspondence to Professor James Barber, Department of Mechanical Engineering and Applied Mechanics, University of Michigan, Ann Arbor, MI 48109. E-mail: jbarber@engin.umich.edu

Journal of Thermal Stresses, 21:309–326, 1998

0149-5739/98 $12.00 + .00

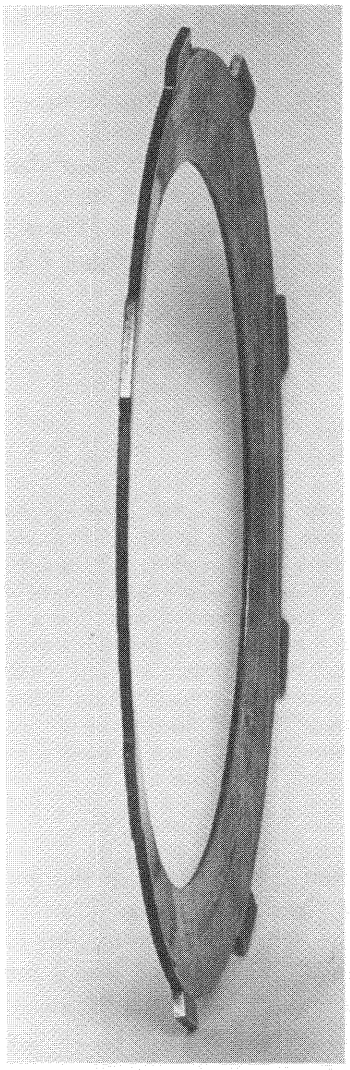

Figure 1. Coning buckling mode for a transmission clutch disk.

inner to outer radius, relief of residual stress causes the cut to open so that the resulting ring has an increased radius but subtends less than 360°. By contrast, a disk distorted into the potato chip mode will relax up on cutting into a *reduced* radius and will overlap at the cut to subtend *more* than 360°.

Both forms typically revert to a plane shape when the in-plane residual stress is released in this way, showing that the deformation is the result of buckling rather than out-of-plane residual stress.

In-plane thermal stresses can be expected whenever there is a temperature difference between the inner and outer radii of the disk. The discolored bands in Figure 2(*b*) show clear evidence of such temperature differences and suggest an

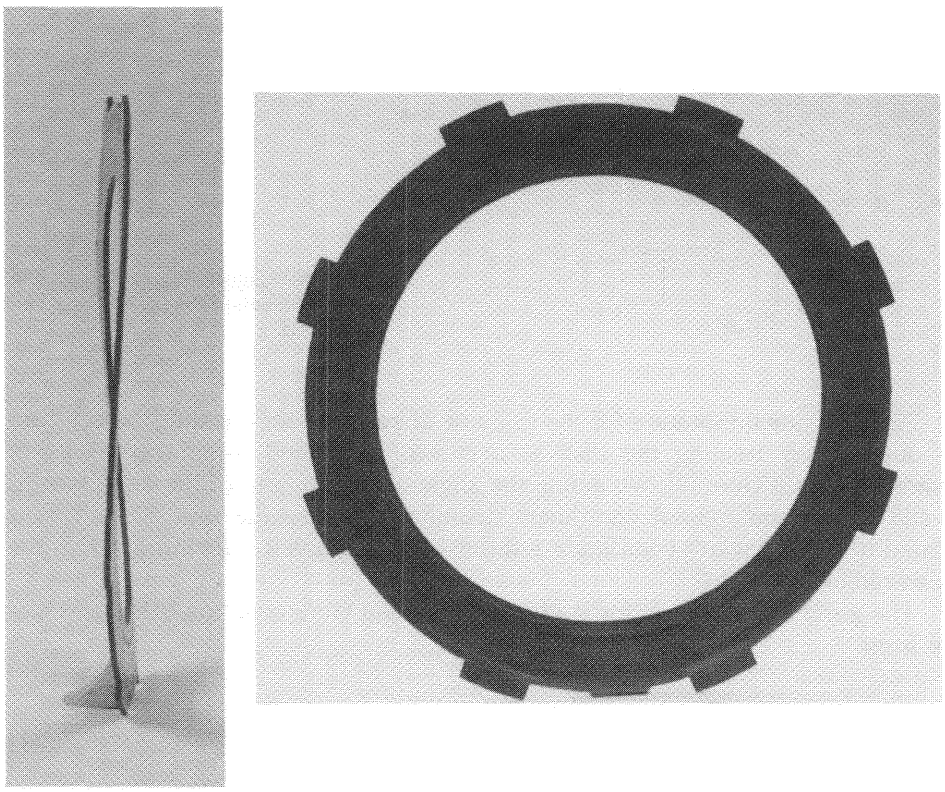

(*a*) (*b*)

Figure 2. Potato chip ($N = 2$) mode.

approximately axisymmetric temperature distribution even though the disk buckled in the $N = 2$ mode. Various authors [4–8] have shown that nonuniform heating at sliding surfaces can be caused by frictionally excited *thermoelastic instability* (TEI), whereby thermoelastic distortions of the sliding bodies affect the contact pressure distribution, exaggerating any initial nonuniformity and leading eventually to incomplete contact between the surfaces.

THEORETICAL CRITICAL MOMENT M_0

Consider a scenario in which the thermal history is at all times axisymmetric, leading to an axisymmetric state of residual stress. The residual stress must satisfy global equilibrium conditions; hence, the only force resultant that can be transmitted across a typical disk section is an in-plane bending moment M, as shown in Figure 3, which also defines a sign convention for M.

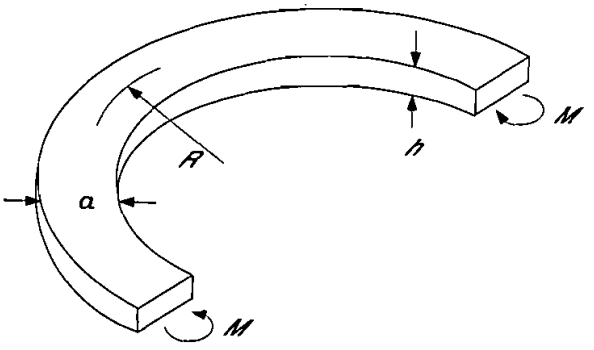

Figure 3. Dimensions of the disk and sign convention for the in-plane moment, M.

An approximate solution for the value of M required for buckling to occur can be obtained by treating the disk as a curved beam and using the results of Timoshenko and Gere [9]. We define the angle of rotation out of the disk plane as ϕ and the circumferential coordinate defining points on the disk as θ. This is related to Timoshenko's coordinate s through the relation $s = R\theta$, where R is the mean radius of the disk.

The governing equation for ϕ (Timoshenko and Gere equation (h)) then takes the form

$$\frac{d^2\phi}{d\theta^2} + N^2\phi = 0 \tag{1}$$

where

$$N^2 = \frac{R^2}{EIC}\left(M_0 - \frac{C}{R}\right)\left(M_0 - \frac{EI}{R}\right) \tag{2}$$

and EI, C are the rigidities in out-of-plane bending and torsion, respectively, for the disk cross section. For a complete disk, Eq. (1) has nontrivial solutions only when N is an integer, which defines the number of waves around the circumference in the deformation mode.

A more convenient dimensionless form of Eq. (2) can be obtained by defining

$$\tilde{M} \equiv \frac{MR}{C} \qquad K \equiv \frac{EI}{C} \tag{3}$$

giving

$$N^2 = \frac{\left(\tilde{M}_0 - K\right)\left(\tilde{M}_0 - 1\right)}{K} \tag{4}$$

Solving for the dimensionless critical moment $\tilde{M}_0$, we obtain

$$\tilde{M}_0 = \frac{1+K}{2} \pm \sqrt{\left(\frac{1-K}{2}\right)^2 + KN^2} \tag{5}$$

giving two solutions for each integer value of N.

The stiffness ratio K is generally less than unity. For the special case of a rectangular cross section of thickness h and radial thickness a (see Figure 3), we have

$$I = \frac{ah^3}{12} \qquad C = \frac{Gah^3}{3} \tag{6}$$

and hence

$$K = \frac{1+\nu}{2} \tag{7}$$

from (3, 6), where ν is Poisson's ratio and we have used the fact that the shear modulus $G = E/2(1+\nu)$.

In general, the critical moments increase with N, so only the first few modes are of practical importance. Figure 4 shows the two solutions of Eq. (5) as functions of ν for $N = 0, 1, 2$. One of the solutions for $N = 1$ is a rigid-body mode ($\tilde{M}_0 = 0$)

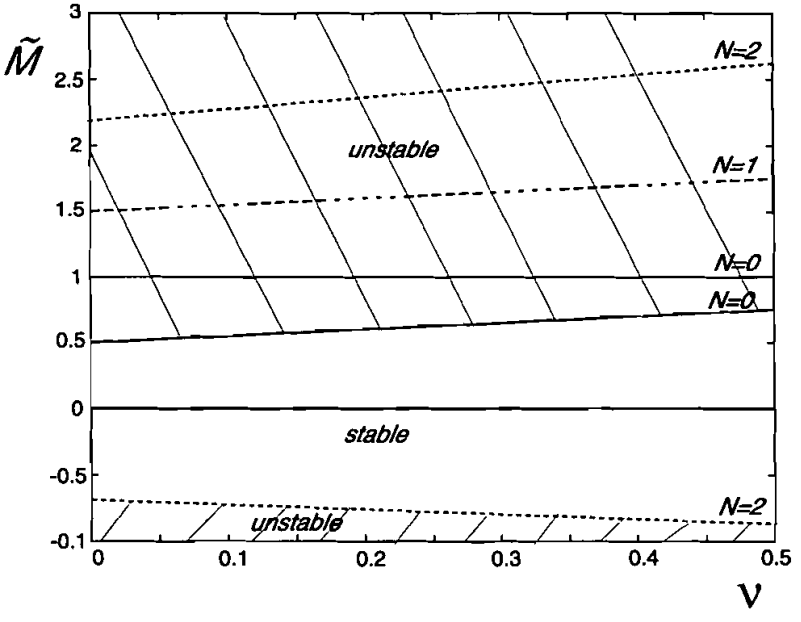

Figure 4. The critical dimensionless bending moment, $\tilde{M}$, in the first three modes.

and does not affect the elastic stability of the system. For all values of ν, the stability boundary is determined by an axisymmetric ($N = 0$) mode if $\tilde{M} > 0$ and by the $N = 2$ mode if $\tilde{M} < 0$. The stable range for $\tilde{M}$ is therefore defined by

$$\frac{1+K}{2} - \sqrt{\left(\frac{1-K}{2}\right)^2 + 4K} < \tilde{M} < K \tag{8}$$

In dimensional terms, the critical moments are related to $\tilde{M}_0$ through

$$M_0 = \frac{\tilde{M}_0 C}{R} = \frac{\tilde{M}_0 G a h^3}{3R} \tag{9}$$

Table 1 shows the corresponding values of critical moment M for steel disks ($G = 80$ GPa, $\nu = 0.3$) of dimensions $a = 30$ mm and $R = 125$ mm and two different thicknesses $h = 2$ mm and $h = 3$ mm. Notice that the magnitude of the moment required for the potato chip mode is slightly larger than that for coning, but both values are very sensitive to the disk thickness because of the presence of the term h^3 in Eq. (9).

These results show that in-plane residual stresses can cause buckling of clutch disks in coning or potato chip modes depending on the sign of the residual moment and that they agree closely with qualitative aspects of experimental observations reported in the introduction. To be able to make a more quantitative comparison, we need to be able to predict the residual in-plane moment that will be produced as a result of a given axisymmetric thermal history. This question will be addressed in the next section.

EFFECT OF THERMAL HISTORY ON RESIDUAL MOMENT

Figure 5 shows a section through the annular disk. We assume that the normal stress σ is a function of the radial coordinate y only; that is, there is no variation in stress through the thickness and the stress field is axisymmetric.

Table 1 Critical moments

	$N = 0$ (coning)	$N = 2$ (potato chip)
$\tilde{M}$	0.65	−0.797
M ($h = 2$ mm)	33.280 Nm	−40.806 Nm
M ($h = 3$ mm)	112.320 Nm	−137.721 Nm

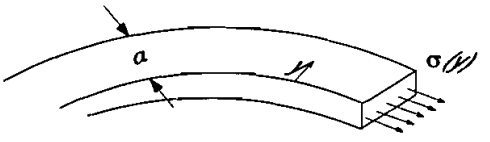

Figure 5. In-plane stress in the disk.

If the surfaces of the disk are traction-free, there must be no net circumferential force in the disk and hence the stress must satisfy the equilibrium equation

$$F = \int_0^a \sigma(y) h \, dy = 0 \tag{10}$$

However, the section can transmit an axisymmetric moment that is defined by

$$M = \int_0^a \sigma(y) h y \, dy \tag{11}$$

We assume that the disk is subjected to a temperature field $T(y,t)$, where t is time, causing a thermal stress field, $\sigma(y,t)$, that satisfies Eq. (10). The stress is limited in value by the yield stress of the material, $S_Y(T)$, which depends on the material but is also generally a decreasing function of temperature. Nonlinearity is also introduced into the problem by the significant temperature dependence of (i) the thermal expansion coefficient $\alpha(T)$ and (ii) Young's modulus $E(T)$ over the practical range of operating temperatures.

Uniform Stress Solution

We first consider the simpler problem of a one-dimensional bar in which the stress $\sigma(t)$ is uniform (independent of y) and the strain $e(t)$ and temperature $T(t)$ are prescribed functions of time.

These quantities are related by the equation

$$e(t) = \frac{\sigma(t)}{E(T)} + \int_0^T \alpha(T) \, dT + e_p(t) \tag{12}$$

where $e_p(t)$ is the value of plastic strain at time t. We assume that the initial plastic strain is zero, that is, $e_p(0) = 0$.

At any given time, the bar must be either (i) yielding in tension with $\sigma(t) = S_Y(T(t))$; (ii) yielding in compression with $\sigma(t) = -S_Y(T(t))$; or (iii) deforming elastically, in which case $de_p/dt = 0$. Thus, if the bar stays in the same state throughout a small time increment dt, we can solve for the plastic strain $e_p(t)$ in cases (i), (ii) and for the unknown stress $\sigma(t)$ in case (iii).

One-dimensional algorithm. An algorithm was developed to implement these conditions and predict the evolution of stress $\sigma(t)$ for given values of $e(t)$ and $T(t)$.

Suppose that the plastic strain $e_p(t)$ is known at time t. After a small increment of time, δt, we know the new values of strain $e(t + \delta t)$ and temperature $T(t + \delta t)$ and, hence, can calculate the stress $\sigma(t + \delta t)$ from Eq. (12) under the assumption that the bar remains elastic, that is, that e_p remains unchanged.

We compare this result with the yield stress $S_Y(T)$ corresponding to $T(t + \delta t)$.

- If $-S_Y < \sigma < S_Y$ the assumption of elastic deformation is correct and we proceed to the next time increment.
- If $\sigma > S_Y$, the bar yields in tension. We therefore set $\sigma = S_Y$ and solve Eq. (12) for $e_p(t + \delta t)$ obtaining

$$e_p(t + \delta t) = e(t + \delta t) - \frac{S_Y(T)}{E(T)} - \int_0^T \alpha(T)\, dT \tag{13}$$

- If $\sigma < -S_Y$, the bar yields in compression. We set $\sigma = -S_Y$ and solve Eq. (12) for $e_p(t + \delta t)$ obtaining

$$e_p(t + \delta t) = e(t + \delta t) + \frac{S_Y(T)}{E(T)} - \int_0^T \alpha(T)\, dT \tag{14}$$

Material properties. For these calculations, we need experimental data describing the variation of material properties with temperature. Figure 6 shows Young's modulus E, yield stress S_Y, and thermal expansion coefficient α as functions of temperature for AISI 1020 steel [10]. In the preceding algorithm, these values were input at a set of discrete points and intermediate values were obtained by interpolation.

One-dimensional example. The one-dimensional algorithm was tested using a variety of scenarios for $T(t), e(t)$. For example, Figure 7 shows the stress history when the strain is held constant at $e(t) = 0$ and the temperature first increases to a maximum of 600°C and then decreases. As the temperature increases, thermal expansion is prevented, leading to a compressive (negative) stress. Yielding occurs at A and the compressive stress decreases between A and B because the yield stress falls with increasing temperature. Cooling starts at B and the deformation is elastic between B and C, at which point the tensile yield stress is reached. The stress rises slowly during the plastic deformation between C and D due to the increase in yield stress with falling temperature.

The Annular Disk

We now return to the annular disk of Figures 3 and 5. To obtain an approximate solution for the residual stress, we divide the radial thickness a into N equal

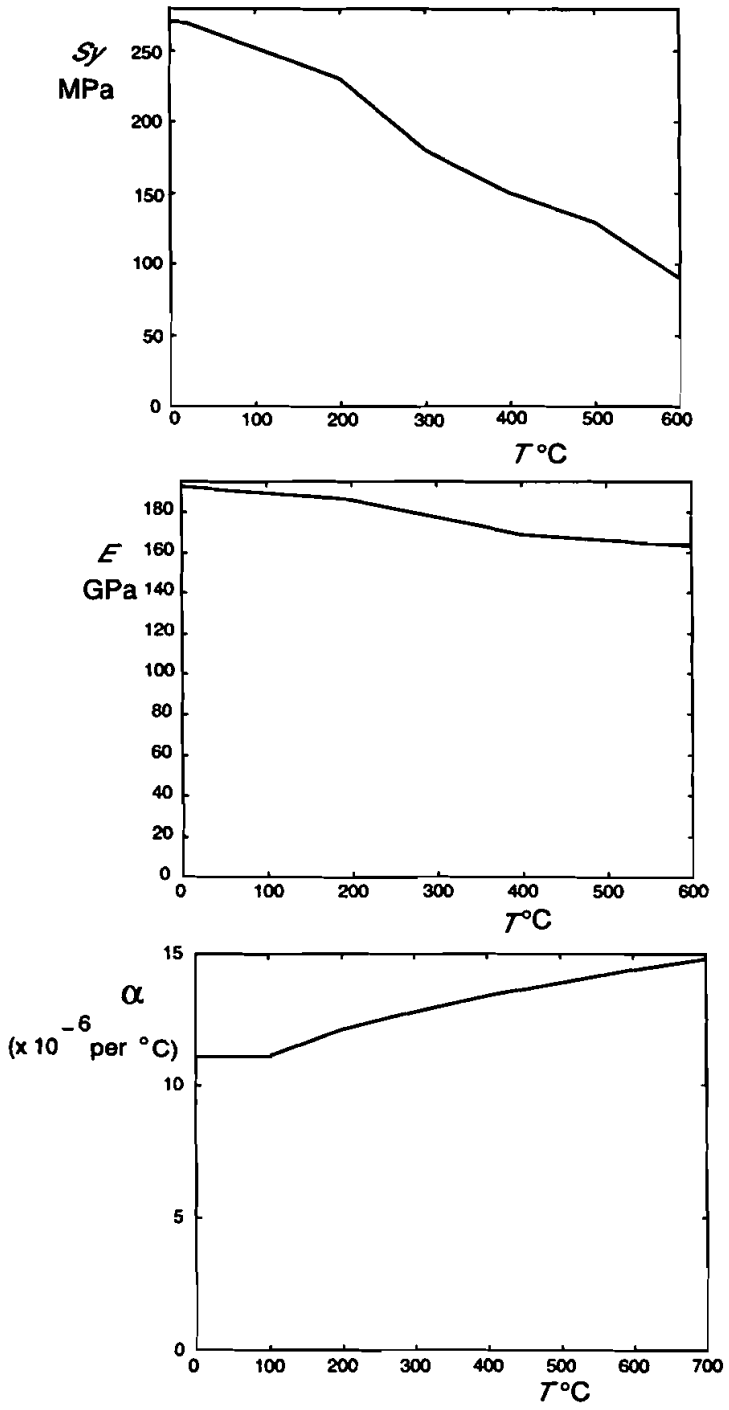

Figure 6. Effect of temperature on yield strength S_Y, Young's modulus E, and thermal expansion coefficient α for AISI 1020 steel (from [10]).

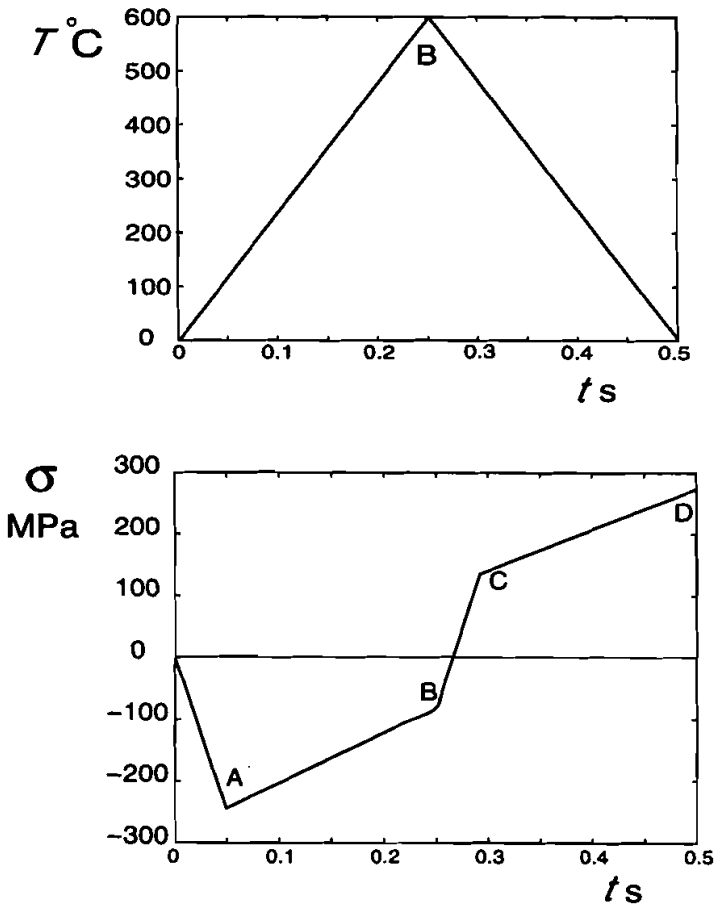

Figure 7. Stress history for a one-dimensional example in which the strain $e(t) = 0$.

elements of length

$$\delta y = \frac{a}{N} \tag{15}$$

in each of which the stress is assumed to be constant.

The stress σ_i in element i satisfies the equation

$$e_i(t) = \frac{\sigma_i(t)}{E(T_i)} + \int_0^{T_i} \alpha(T_i)\, dT_i + e_{pi}(t) \tag{16}$$

from Eq. (12), where T_i is the temperature in element i.

The resultant force in element i

$$F_i = \frac{ah\sigma_i}{N} \tag{17}$$

acts through the midpoint of the element at

$$y_i = \frac{a(2i-1)}{2N} \tag{18}$$

Determination of strain. The ring is free to expand, so the strain $e(t)$ is unknown, but it is the same for all the elements. To determine it we have the equilibrium equation (10), which, with Eq. (17) gives

$$F = \sum_{i=1}^{N} F_i = \sum_{i=1}^{N} \frac{ah\sigma_i}{N} = 0 \tag{19}$$

or

$$\sum_{i=1}^{N} \sigma_i = 0 \tag{20}$$

We calculate $e(t)$ at each time step by iteration. The iteration will be considered to be converged when F as defined by Eq. (19) is sufficiently small. For this purpose, we define the function

$$S_t = \sum_{i=1}^{N} \frac{\sigma_i}{S_Y(0)N} = \frac{F}{ahS_Y(0)} \tag{21}$$

which is a measure of the error in force F. Notice that the maximum value of $|S_t|$ is 1 because

$$|\sigma_i| \le S_Y(T(t)) \le S_Y(0) \tag{22}$$

Adequate convergence therefore requires that $|S_t| \ll 1$. In the following examples, tests were conducted defining convergence at $|S_t| = 10^{-2}, 10^{-3} \ldots$.

Iteration algorithm. As an initial guess, we use the value of $e(t)$ at the previous time step or zero for the first time step.

At any given stage in the iteration, the sensitivity of the force F to the strain e can be defined as

$$\frac{dF}{de} = \frac{ha}{N} \sum_{i=1}^{N} (1 - s_i^2) E(T_i) \tag{23}$$

where $s_i = 0$ for those elements that are in the elastic range, $s_i = 1$ for those that are yielding in tension, and $s_i = -1$ for those that are yielding in compression. For the next iteration, we therefore choose

$$e_{k+1} = e_k - \frac{NS_Y(0)S_t}{\sum_{i=1}^{N}(1 - s_i^2)E(T_i)} \tag{24}$$

This strategy converges rapidly as long as there is at least one element that remains elastic, but Eq. (24) becomes unbounded if all the elements are yielding. This can arise in two ways.

1. If the number of elements used, N, is small, severe thermal loading may predict that some yield in tension and the remainder in compression, without an intervening elastic zone. In practice, this means that the size of the elastic zone that would be obtained in a continuum solution is significantly smaller than the discretization δ. When this condition is detected, the singularity can be avoided by setting a minimum value to dF/de; for example, by replacing Eq. (24) by

$$e_{k+1} = e_k - \frac{N^2 S_Y(0)S_t}{\sum_{i=1}^{N}E(T_i)} \tag{25}$$

   which corresponds to the assumption of one elastic element with the average value of $E(T)$ over all the elements.
2. If a large time step is used, so that the temperature changes significantly during δt, the initial guess $e(t + \delta t) = e(t)$ may result in a prediction that all elements yield in the same direction (tension or compression). In this case, the final state is likely to involve elastic conditions at many elements, so an appropriate modification of Eq. (24) would be to assume that *all* the elements are elastic, giving

$$e_{k+1} = e_k - \frac{NS_Y(0)S_t}{\sum_{i=1}^{N}E(T_i)} \tag{26}$$

   Alternatively, the problem can be corrected simply by reverting to a smaller time step.

The moment. Once e and hence σ_i are known, the moment M can be found from Eq. (11), which in discrete form can be written as

$$M = \sum_{i=1}^{N} F_i y_i = \frac{a^2 h}{2N^2} \sum_{i=1}^{N} (2i - 1)\sigma_i \tag{27}$$

It is convenient to define a dimensionless moment using the notation of Eqs. (3) and (9). We obtain

$$\tilde{M} = \frac{3RM}{Gah^3} = \frac{3\psi}{2GN^2} \sum_{i=1}^{N} (2i-1)\sigma_i \tag{28}$$

where G is the shear modulus at room temperature and the geometric shape factor

$$\psi = \frac{aR}{h^2} \tag{29}$$

The disk dimensions enter Eq. (28) only through the factor ψ and the critical value $\tilde{M}_0$ for buckling depends only on Poisson's ratio and is given in Figure 4. We conclude that for a given thermal history, there will be a critical value of ψ above which buckling will occur on cooling. Typical design values of ψ for both automotive and construction machinery transmissions lie in the range $250 < \psi < 600$.

Results

To illustrate the operation of the program and to investigate the convergence and stability of the results, we first consider a steel disk of radial thickness $a = 30$ mm and thickness $h = 3$ mm subjected to the temperature profile

$$T(y,t) = \frac{1800ty}{a} \qquad 0 < t < 0.25 \tag{30}$$

$$= \frac{1800(0.5-t)y}{a} \qquad 0.25 < t < 0.5 \tag{31}$$

Thus, the temperature at $y = 0$ is always zero and there is a linear variation in temperature through the radial thickness with a maximum temperature difference of 450°C occurring at the outer radius $y = a$. The temperature $T(a,t)$ at the outer radius is shown in Figure 8.

Figure 9 shows the stress field $\sigma(y,t)$ at three instants corresponding to the points A, B, C in Figure 8. The final residual stress field (curve C) shows that the disk has yielded in compression (leaving residual tension) at the outer radius and in tension at the inner radius. The constant stress region near the middle of the section remained elastic throughout the process. The plastic zone at the outer radius is larger than that at the inner radius because the higher temperature there caused a reduction in yield stress. This asymmetry also causes the residual stress in the central elastic zone to differ slightly from zero.

The residual stress state corresponds to a positive residual moment M of about 96.9 Nm, which is lower than the critical value for this thickness (112.3 Nm) from Table 1. Thus, the temperature history considered in this example will not lead to buckling of the disk upon cooling.

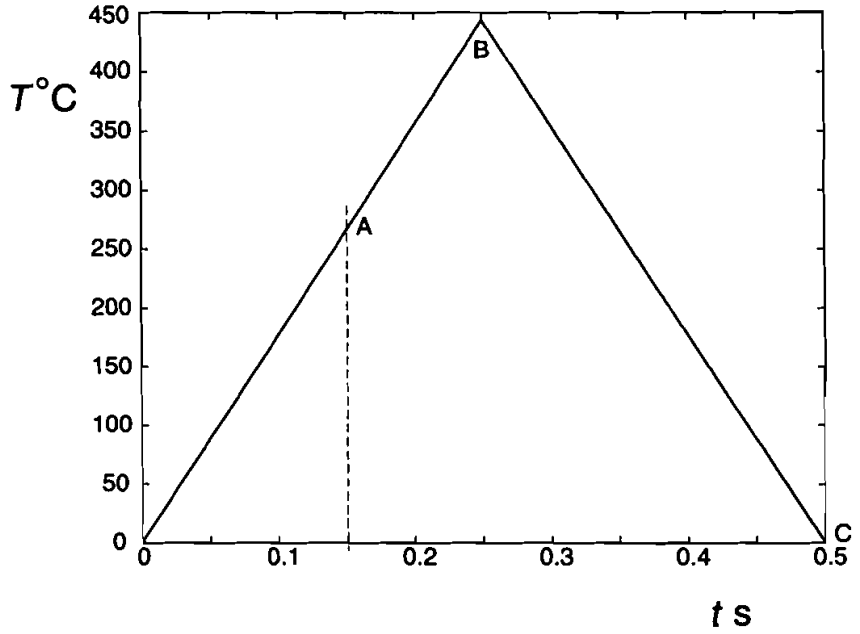

Figure 8. Example 1: Temperature variation at the outer radius, $y = a$.

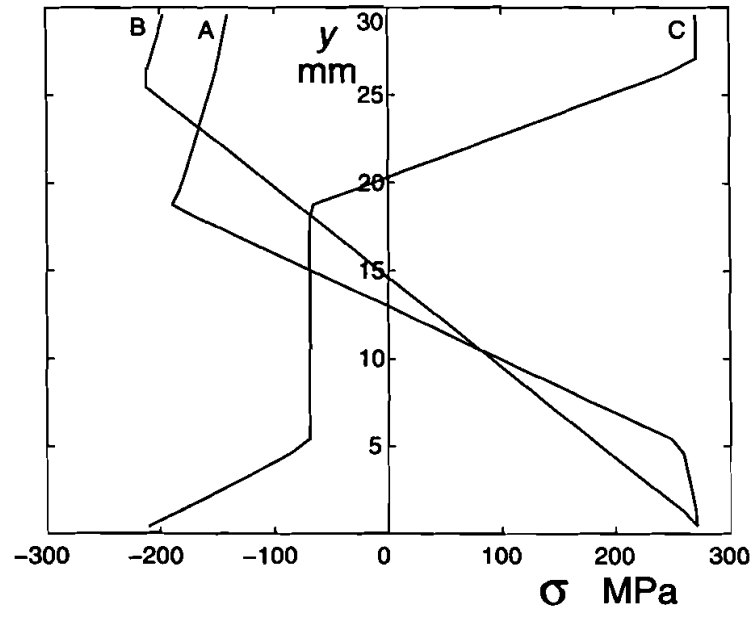

Figure 9. Example 1: Stress fields at t_A, t_B, t_C.

In dimensionless terms, we obtain $\tilde{M} = 0.00135\psi$ and, since the critical dimensionless moment for steel is $\tilde{M}_0 = 0.65$, conclude that buckling would occur in the coning mode for the temperature field of Eqs. (30) and (31) if $\psi > 483$.

Convergence. We might anticipate that the accuracy of the results would be increased by increasing the number of elements N, reducing the time step δt, and reducing the threshold value of $|S_t|$ for convergence as defined by Eq. (21). Tests were conducted to examine the effect of these parameters on the residual moment M in the preceding example.

Initial results appeared to indicate that the time step δt had no effect on the residual moment. Indeed, a solution obtained using just two time steps ($\delta t = 0.25$ sec) gave exactly the same result as those with much smaller values. This occurs because the final moment is only affected by the plastic strain that has occurred during the process, and this in turn is determined by the extreme conditions of temperature. In effect, early yielding of the disk is overlaid by the more extreme yielding that occurs at the instant $t = 0.25$ sec and as long as a time step is chosen that is an integer submultiple of this value, the same final moment is obtained.

In more complex examples, it will not necessarily be clear which points in the time history constitute defining events for the final plastic strain; hence a time step must be chosen that will capture such events sufficiently closely to give acceptable accuracy. With this in mind, we used an odd number of time steps in order to ensure that the instant $t = 0.25$ sec would occur midway through a time step. The corresponding residual moment is given in Table 2 for various values of $|S_t|$ and δt.

The results show that three-digit accuracy can be obtained with $\delta t = 5 \times 10^{-5}$ sec and $|S_t| < 10^{-3}$. Since the source of the approximation lies in the fact that the maximum temperature point is not exactly located, a more appropriate description of this criterion is to note that after convergence *the maximum change in temperature during one time step at any location is* 0.1°C.

Effect of N. A series of runs was conducted using $\delta t = 10^{-2}$, $S_t = 10^{-3}$, and various numbers of elements N through the radial thickness. The results showed that convergence to three significant digits (96.9 Nm) occurred for $N \geq 60$.

Summary. Based on these results and similar tests with other examples, we found that three-digit accuracy can be achieved using the values $S_t = 10^{-3}$ and $N = 60$

Table 2 Effect of δt and $|S_t|$ on the predicted residual moment (Nm)

S_t / δt	10^{-2}	10^{-3}	10^{-4}	10^{-5}	10^{-6}
0.5/9	74.339	73.768	73.738	73.710	73.709
0.5/101	96.508	95.077	94.995	94.987	94.986
0.5/1001	97.257	96.844	96.726	96.717	96.716
0.5/10001	99.534	97.175	96.904	96.894	96.893
0.5/50001	100.467	97.245	96.936	96.911	96.911

and choosing δt such that the maximum change in temperature during one time step at any location is 0.1°C. Two-digit accuracy can be achieved using $S_t = 10^{-3}$, $N = 12$, and a maximum temperature change per time step of 0.7°C.

Additional examples. Using these convergence criteria, results were obtained for a variety of different temperature scenarios. The second case was similar to that of Figure 8 except that the maximum temperature at $y = a$ was increased to 622.5°C, that is,

$$T(y,t) = \frac{2490ty}{a} \qquad 0 < t < 0.25 \tag{32}$$

$$= \frac{2490(0.5-t)y}{a} \qquad 0.25 < t < 0.5 \tag{33}$$

The resulting stress fields are broadly similar to those of Figure 9, with of course a greater amount of plastic deformation, and the final dimensionless residual moment is 0.00206ψ, which is sufficient to cause buckling in the coning ($N = 0$) mode if $\psi > 316$. If y in Eqs. (32) and (33) is replaced by $(a - y)$, the temperature field will be reversed with the high-temperature excursion occurring at the *inner* radius. In that case, a negative moment of equal magnitude will be produced and buckling will occur in the potato chip mode if $\psi > 386$.

Figure 10 shows a scenario in which there is first a temperature excursion at the inner radius $y = 0$ to a maximum of 600°C. The temperature at $y = 0$ then falls, while that at the outer radius $y = a$ increases, also to a maximum of 600°C. Finally, the disk cools back to zero temperature, that is,

$$T(y,t) = \frac{4800ty}{a} \qquad 0 < t < 0.125 \tag{34}$$

$$= \frac{4800(0.25-t)y}{a} + \frac{4800(a-y)(t-0.125)}{a} \qquad 0.125 < t < 0.25 \tag{35}$$

$$= \frac{4800(a-y)(0.375-t)}{a} \qquad 0.25 < t < 0.375 \tag{36}$$

Figure 11 shows the stress distributions obtained at the points A, B, C. The final dimensionless residual moment is -0.00195ψ, which is sufficient to cause buckling in the potato chip mode if $\psi > 333$.

CONCLUSIONS

The preceding results show that transmission clutch plates subjected to axisymmetric temperature excursions can develop residual in-plane bending moments of sufficient magnitude to cause buckling on unloading. Axisymmetric buckling (con-

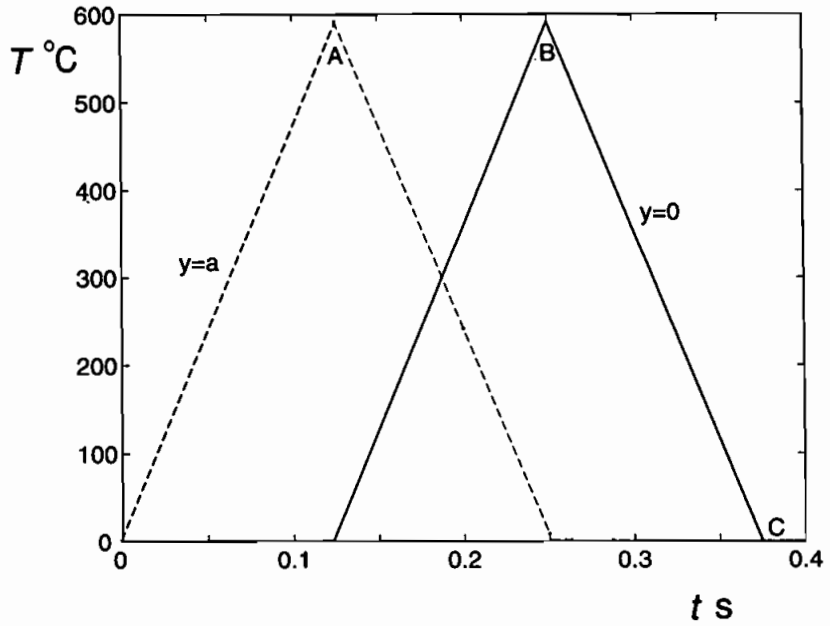

Figure 10. Example 2: Temperature variation at the inner and outer radii $y = 0, a$.

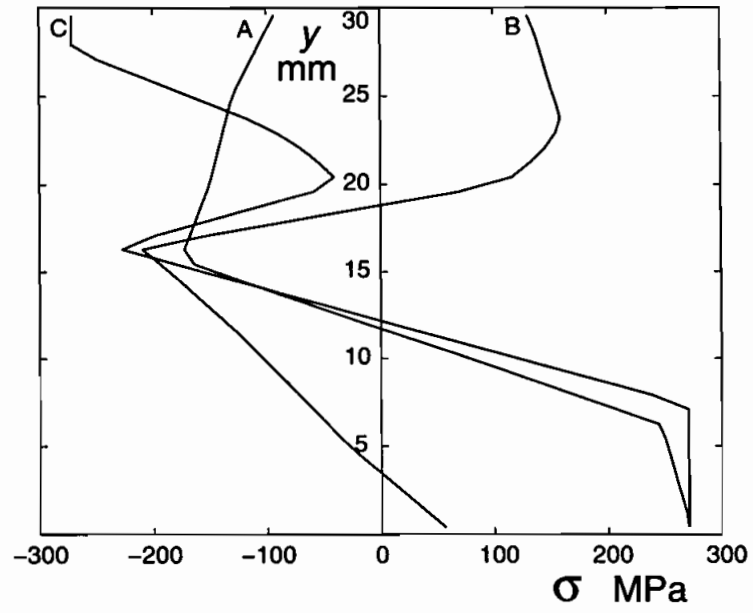

Figure 11. Example 2: Stress fields at t_A, t_B, t_C.

ing) occurs when the residual stress at the outer radius is tensile and a nonaxisymmetric ($N = 2$) potato chip mode occurs when it is compressive. Note that the nonaxisymmetric mode is caused by an *axisymmetric* residual stress field.

Susceptibility to buckling increases with the dimensionless shape factor $\psi = aR/h^2$. Typical design values of ψ for both automotive and construction machinery transmissions lie in the range $250 < \psi < 600$. At the upper end of this range, disks of AISI 1020 steel can achieve residual moments sufficient for buckling with temperature excursions of the order of 450°C, whereas for $\psi = 350$ temperatures must exceed 600°C for buckling to occur.

REFERENCES

1. H. Straub, Der Lamellenverschleiss als Lebensdauergrenze, *VDI-Berichte*, vol. 73, pp. 81–87, 1963.
2. T. P. Newcomb and R. T. Spurr, The Interaction Between Friction Materials and Lubricants, *Wear*, vol. 24, pp. 69–76, 1973.
3. P. Zagrodzki, Numerical Analysis of Temperature Fields and Thermal Stresses in the Friction Disks of a Multidisc Wet Clutch, *Wear*, vol. 101, pp. 255–271, 1985.
4. J. R. Barber, Thermoelastic Instabilities in the Sliding of Conforming Solids, *Proc. Roy. Soc.*, vol. A312, pp. 381–394, 1969.
5. T. A. Dow and R. A. Burton, Thermoelastic Instability of Sliding Contact in the Absence of Wear, *Wear*, vol. 19, pp. 315–328, 1972.
6. F. E. Kennedy and F. F. Ling, A Thermal, Thermoelastic and Wear Simulation of a High Energy Sliding Contact Problem, *ASME J. Lub. Tech.*, vol. 96, pp. 497–507, 1974.
7. P. Zagrodzki, Analysis of Thermomechanical Phenomena in Multidisc Clutches and Brakes, *Wear*, vol. 140, pp. 291–308, 1990.
8. Shuqin Du, P. Zagrodzki, J. R. Barber, and G. M. Hulbert, Finite Element Analysis of Frictionally-Excited Thermoelastic Instability, *J. Thermal Stresses*, vol. 20, pp. 185–201, 1997.
9. S. P. Timoshenko and J. M. Gere, *Theory of Elastic Stability*, McGraw-Hill, New York, 1961, §7.10.
10. *ASM Metals Handbook, Vol. 1*, 9th ed., pp. 641–644, American Society for Metals, Metals Park, OH, 1981.